Available online at www.sciencedirect.com
ScienceDirect
Polymer 48 (2007) 2768–2777
polymer
www.elsevier.com/locate/polymer

Mechanical properties, morphologies, and crystallization behavior of plasticized poly(L-lactide)/poly(butylene succinate-*co*-L-lactate) blends

Mitsuhiro Shibata*, Naozumi Teramoto, Yusuke Inoue

Department of Life and Environmental Sciences, Faculty of Engineering, Chiba Institute of Technology, 2-17-1 Tsudanuma, Narashino, Chiba 275-0016, Japan

Received 29 March 2006; received in revised form 1 February 2007; accepted 25 February 2007
Available online 2 March 2007

Abstract

The blends of poly(L-lactide) (PLLA) with poly(butylene succinate-*co*-L-lactate) (PBSL) containing the lactate unit of *ca*. 3 mol% and Rikemal PL710 (RKM) which is a plasticizer mainly composed of diglycerine tetraacetate were prepared by melt-mixing and subsequent injection molding. The studied RKM content of the PLLA/PBSL/RKM blends was 0–20 wt%, and the PLLA/PBSL weight ratio was 100/0 to 80/20. Although elongation at break in the tensile test did not increase by the addition of 10 wt% RKM to PLLA, the addition of a small amount of PBSL to the PLLA/RKM blend caused a considerable increase of the elongation. The SEM and DSC analyses revealed that all the PLLA/PBSL/RKM blends are immiscible blends where the PBSL particles are finely dispersed, and that there is some compatibility between PLLA-rich phase and PBSL-rich phase in the amorphous state when the RKM content is 20 wt%. As a result of investigation of the crystallization behavior by DSC and polarized optical microscopic measurements, it was revealed that the addition of RKM causes the acceleration of crystalline growth rate at a lower annealing temperature, and the addition of PBSL mainly enhances the formation of PLLA crystal nucleus.
© 2007 Elsevier Ltd. All rights reserved.

Keywords: Blends of poly(L-lactide); Plasticizer; Poly(butylene succinate-*co*-L-lactate)

1. Introduction

Poly(L-lactide) (PLLA) has received a lot of attention in respect that it can be derived from renewable resources such as corn or sugarcane, in addition to its biodegradability [1–7]. Also, the quantity of carbon dioxide generation by the incineration of PLLA is much less than those of conventional petrochemical plastics such as polystyrene, polyethylene, and polypropylene [8]. However, its brittleness is a major defect in the case of attempting to expand uses for packaging applications. Considerable efforts have been made to improve the properties of PLLA so as to complete with low-cost and flexible petroleum-based polymers. These attempts were carried out by blending PLLA with low-molecular weight plasticizers or by blending with other polymers.

Various types of compounds such as glycerol, ethylene glycol oligomer, citrate ester, glucose monoesters, partial fatty acid esters, lactic acid oligomer, and diglycerine tetraacetate, *etc*. have been reported as plasticizers for PLLA in the literature [9–14]. Among various plasticizers for PLLA, diglycerine tetraacetate is expected to be an excellent one in view of good miscibility with PLLA, efficient reduction of T_g, and relatively good resistance to moisture and hydrolysis. However, as a common defect of the PLLA plasticizers, the migration of plasticizer molecules to a material surface induced by the crystallization of PLLA and phase separation, worsening the material properties, is a practical obstacle to its application as a packaging material. The glass transition temperature (T_g) of the plasticized PLLA is much lower than that of PLLA (60 °C). The cold crystallization of its PLLA component may occur at a temperature not less than the T_g. Therefore, it is difficult to obtain meta-stable plasticized PLLA which does not crystallize at ambient temperature. It is thought that the plasticized PLLA which has already attained

* Corresponding author. Tel.: +81 47 478 0423; fax: +81 47 478 0439.
E-mail address: shibata@sky.it-chiba.ac.jp (M. Shibata).

0032-3861/$ - see front matter © 2007 Elsevier Ltd. All rights reserved.
doi:10.1016/j.polymer.2007.02.065

an ultimate crystallinity on molding is suitable. In this case, it is necessary to enhance the crystallization rate and to use the least amount of plasticizer in order to avoid the phase separation of plasticizer accompanied by the PLLA crystallization.

On the other hand, the blending of PLLA with other biodegradable aliphatic polyesters such as poly(butylene succinate) (PBS) [15,16], poly(ε-caprolactone) [17–19], and poly(hydroxybutyrate) [20,21] was also investigated to improve the brittle character. Recently, we reported that the addition of 1–10 wt% poly(butylene succinate-*co*-L-lactate) (PBSL) to PLLA causes a considerable improvement of the brittle character and an increase of the crystallization rate from the melt [22].

In this study, PLLA was blended with PBSL and Rikemal PL710 (RKM) which is a PLLA plasticizer mainly composed of diglycerine tetraacetate, and its mechanical properties, morphologies, and crystallization behaviors were investigated. The purpose of this study is to obtain the PLLA/PBSL/RKM blends having high crystallization rate and good flexibility by using the least amount of RKM.

2. Experimental

2.1. Materials

PLLA (LACEA® H-100, melt flow rate (190 °C, 2.16 kg) 8 g/10 min, specific gravity 1.26) was supplied from Mitsui Chemicals Inc. (Japan). PBSL (GS Pla® AZ-type, lactate unit *ca.* 3 mol%, melt flow rate (190 °C, 2.16 kg) 25 g/10 min, specific gravity 1.26) was supplied from Mitsubishi Chemical Corporation (Japan). As a plasticizer for PLLA, Rikemal PL710 (RKM) which is mainly composed of diglycerine tetraacetate was supplied from Riken Vitamin Co. Ltd.

2.2. Sample preparation

The polymers were dried at 40 °C in a vacuum oven for 24 h before use. Blending of PLLA, PBSL, and RKM was performed using a Laboplasto-Mill with a twin rotary mixer (Toyo Seiki Co. Ltd., Japan). The molten mixing was carried out at 190 °C for all the blends, the rotary speed was 50 rpm, and mixing time was 5 min. The obtained blends were cut into small pieces and again dried at 40 °C in a vacuum oven before the injection molding. The RKM contents in the PLLA/PBSL/RKM blends were 10 and 20 wt%. Weight ratios of PLLA/PBSL were 100/0, 99/1, 95/5, 90/10, and 80/20. For example, the abbreviation PLLA/PBSL5/RKM10 means that weight ratio of the PLLA/PBSL is 95/5 and RKM content in the ternary blend is 10 wt%, that is, the actual PLLA/PBSL/RKM weight ratio is 85.5/4.5/10. Dumbbell-shaped specimens (width 5 mm × thickness 2 mm × length of parallel part 32 mm × total length 72 mm) were molded using a desk injection molding machine (Little-Ace I Type, Tsubako Co. Ltd., Japan). The cylinder temperature and the molding temperature during the injection molding were 190 and 40 °C, respectively. The specimens of PBSL/RKM blends with 10 and 20 wt% RKM were also prepared by the same procedure except that the temperature of mixing and injection cylinder is 140 °C. Film samples of 0.10 mm thick for polarizing optical microscopic analysis were prepared by pressure molding under 0–3 MPa at 190 °C for 4 min and subsequent quenching by ice-water.

2.3. Measurements

Dynamic viscoelastic measurements were performed on a Rheolograph Solid (Toyo Seiki Co., Ltd, Japan) with a chuck distance of 20 mm, a frequency of 10 Hz and a heating rate of 2 °C/min.

The morphology of the blends was observed by field emission-scanning electron microscopy (FE-SEM), using a Hitachi S-4700 machine (Hitachi High-Technologies Corporation, Japan). All samples were fractured after immersion in liquid nitrogen for about 30 min. The fracture surfaces were sputter coated with gold to provide enhanced conductivity.

Tensile tests were performed using an Autograph AG-1 (Shimadzu Co., Ltd., Japan) according to the standard method for testing the tensile properties of rigid plastics (JIS K7113 (1995)). Span length was 50 mm and the testing speed was 10 mm/min. Five composite specimens were tested for each set of samples, and the mean values and standard deviation were calculated.

The differential scanning calorimetric (DSC) measurements were performed on a Perkin–Elmer DSC Pyris 1 DSC in a nitrogen atmosphere. In order to investigate the cold-crystallization behavior of all the blends without the influence of thermal history, all the blends were heated to 190 °C at a rate of 20 °C/min, held at that temperature for 3 min, and then cooled to −10 °C at a cooling rate of 100 °C/min. After that the second heating scans were monitored between −10 and 200 °C at a heating rate of 20 °C/min for determining glass transition temperature (T_g), cold-crystallization temperature (T_c') and melting temperature (T_m). The T_g was obtained as the mid point of the heat capacity change. In the case of the investigation on the effect of cooling rate, the samples were heated to 190 °C at a rate of 100 °C/min, held at that temperature for 3 min, and then cooled at cooling rates of 1, 5, and 20 °C/min. Next, in order to investigate the isothermal crystallization behavior, the blends were heated to 190 °C at a rate of 100 °C/min, held at 190 °C for 3 min, and then cooled to the prescribed crystallization temperature as soon as possible. The heat generated during the development of the crystalline phase was recorded until no further heat evolution was observed, and analyzed according to the usual procedure in order to obtain the relative degree of crystallinity. The relative degree of crystallinity as a function of time was found from Eq. (1):

$$\chi_c(t)/\chi_c(\infty) = \int_{t_0}^{t} (dH/dt)dt \Big/ \int_{t_0}^{\infty} (dH/dt)dt \quad (1)$$

where t_0 is the time at which the sample attains isothermal conditions, as indicated by a flat baseline after the initial spike in the thermal curve, $\chi_c(t)$ is the degree of crystallinity at time t, $\chi_c(\infty)$ is the ultimate crystallinity at very long time, and dH/dt is the heat flow rate.

Optical microscopy was performed on an Olympus BXP polarizing microscope equipped with a Japan High-tech hot-stage RH-350 and a Sony CCD-IRIS color video camera. The sample was heated to 190 °C on the hot-stage, held at 190 °C for 3 min, and cooled to a temperature where the growing of spherulites started.

3. Results and discussion

3.1. Dynamic viscoelastic properties

Figs. 1 and 2 show dynamic viscoelastic curves of PLLA/RKM and PBSL/RKM blends, respectively. For both the blends, the temperature at the maximum of tan δ corresponding to the glass transition temperature of PLLA or PBSL

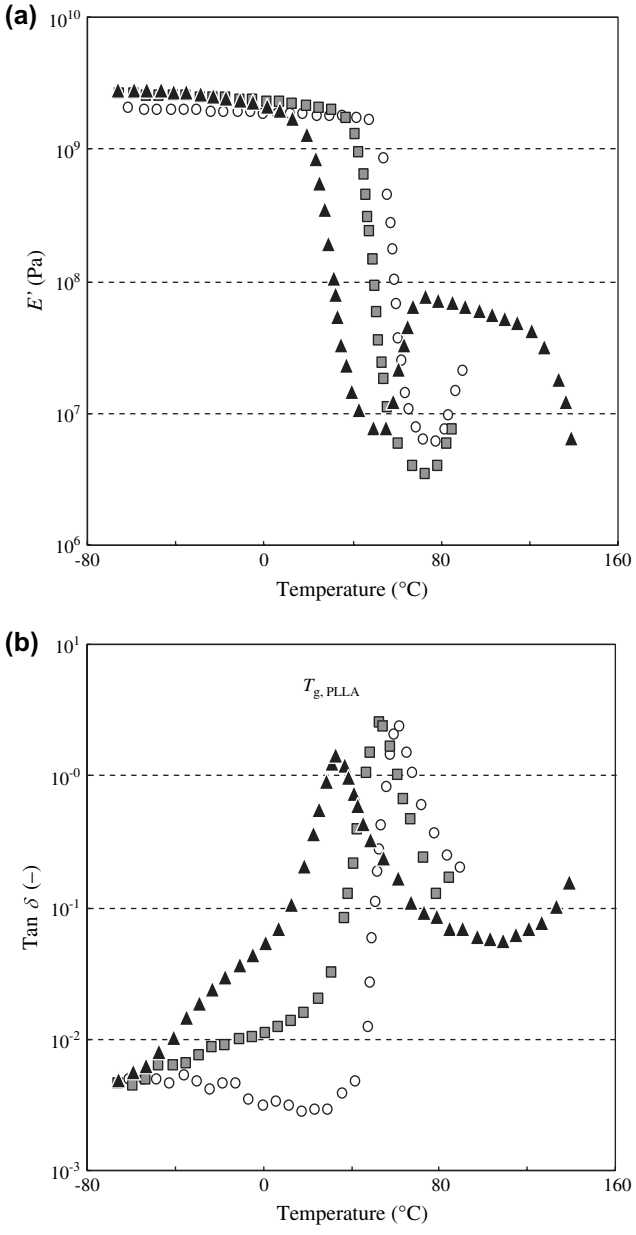

Fig. 1. Dynamic viscoelastic curves of PLLA and PLLA/RKM: (a) E' and (b) tan δ. ○ – PLLA, ■ – PLLA/RKM10, ▲ – PLLA/RKM20.

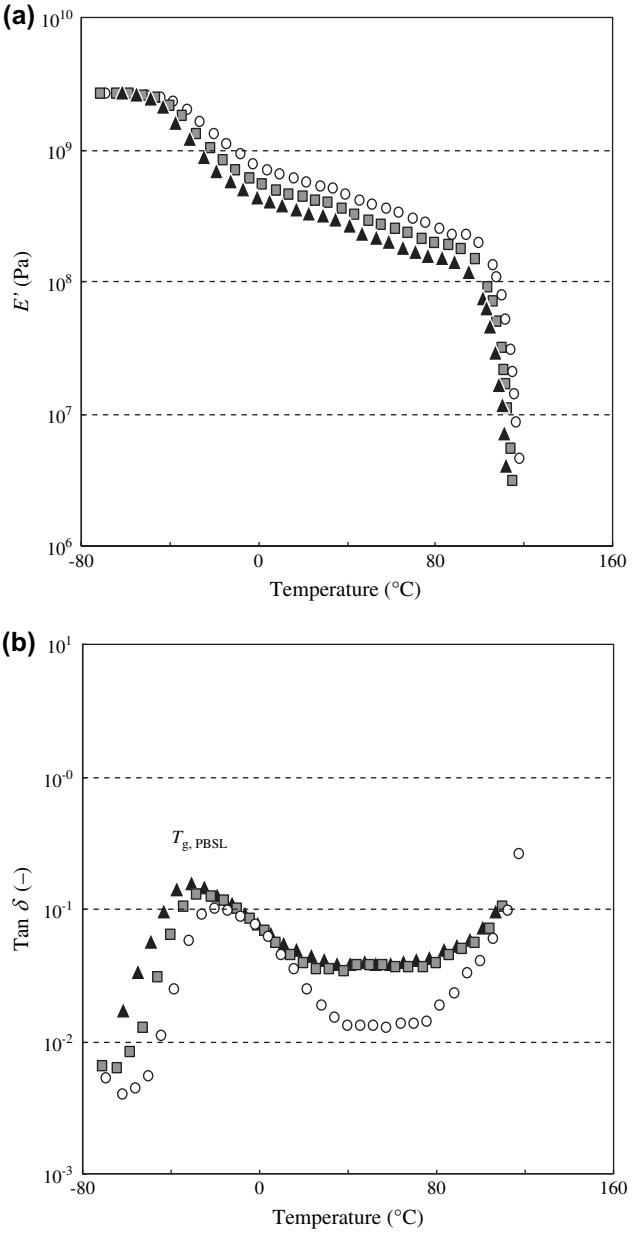

Fig. 2. Dynamic viscoelastic curves of PBSL and PBSL/RKM: (a) E' and (b) tan δ. ○ – PBSL, ■ – PBSL/RKM10, ▲ – PBSL/RKM20.

($T_{g,PLLA}$ or $T_{g,PBSL}$) shifted to a lower temperature region with increasing amount of RKM, indicating that RKM acts as a plasticizer for both PLLA and PBSL. The extent of T_g reduction for PLLA/RKM was much larger than that for PBSL/RKM (Table 1). Also, in the case of PBSL/RKM20, the RKM component bled out from the surface, indicating that RKM is a better plasticizer for PLLA than for PBSL. The storage modulus (E') of PLLA dropped around 50–70 °C due to glass transition, and then rose around 75 °C due to crystallization. In the case of PLLA/RKM, the temperature where E' starts to rise shifted to a lower temperature region with RKM content, indicating that RKM enhances the cold crystallization of PLLA. Such a rise in E' on a heating scan was not observed for PBSL/RKM, because the PBSL/RKM samples had already

Table 1
Glass transition temperatures measured by dynamic viscoelastic measurement for the PLLA/PBSL/RKM and PBSL/RKM blends

RKM content (wt%)	PLLA/PBSL weight ratio of PLLA/PBSL/RKM					PBSL/RKM
	100/0	99/1	95/5	90/10	80/20	$T_{g,PBSL}$ (°C)
	$T_{g,PLLA}$ (°C)					
0	62.1	61.1	58.4	58.1	58.1	−20.0
10	53.1	51.1	50.1	47.2	44.0	−26.8
20	34.1	44.1	42.0	40.0	31.1	−29.9

attained almost the ultimate crystallinity. The E' at the rubbery state decreased with increasing RKM content, although the E' at the glassy state was almost unchanged.

Figs. 3 and 4 show dynamic viscoelastic curves of PLLA/PBSL/RKM10 and PLLA/PBSL/RKM20, respectively. Table 1 summarizes $T_{g,PLLA}$ calculated from the maximum of tan δ peak for PLLA/PBSL blends without RKM in addition to the ternary blend. Because the tan δ peak related to glass transition of PBSL component is very weak and broad, the $T_{g,PBSL}$ could not be read except for PLLA/PBSL20/RKM10 (*ca.* −20 °C). The $T_{g,PLLA}$ of PLLA/PBSL 100/0 to 90/10 binary blends slightly decreased with increasing PBSL content, and became almost constant at 80/20, suggesting that PBSL has a little compatibility with PLLA. In the case of PLLA/PBSL/RKM10, the $T_{g,PLLA}$ slightly decreased with increasing PBSL content in the composition range of the PLLA/PBSL

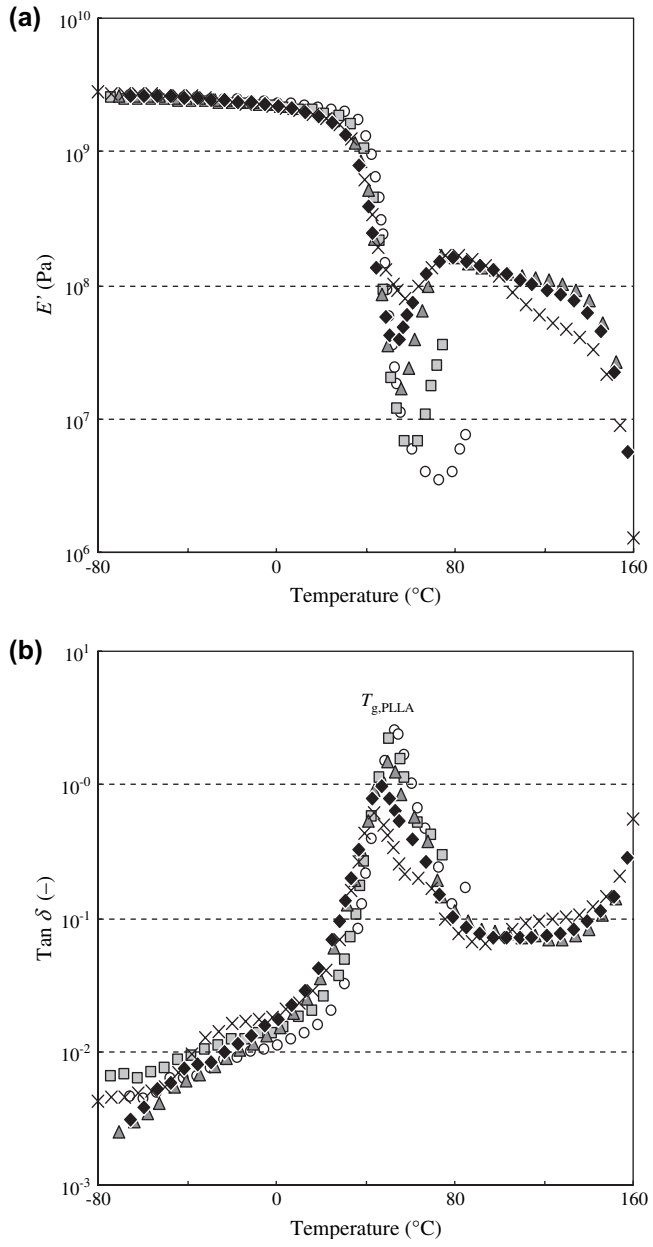

Fig. 3. Dynamic viscoelastic curves of PLLA/RKM10 and PLLA/PBSL/RKM10: (a) E' and (b) tan δ. The PLLA/PBSL weight ratio: ○ − 100/0, ■ − 99/1, ▲ − 95/1, ◆ − 90/10, × − 80/20.

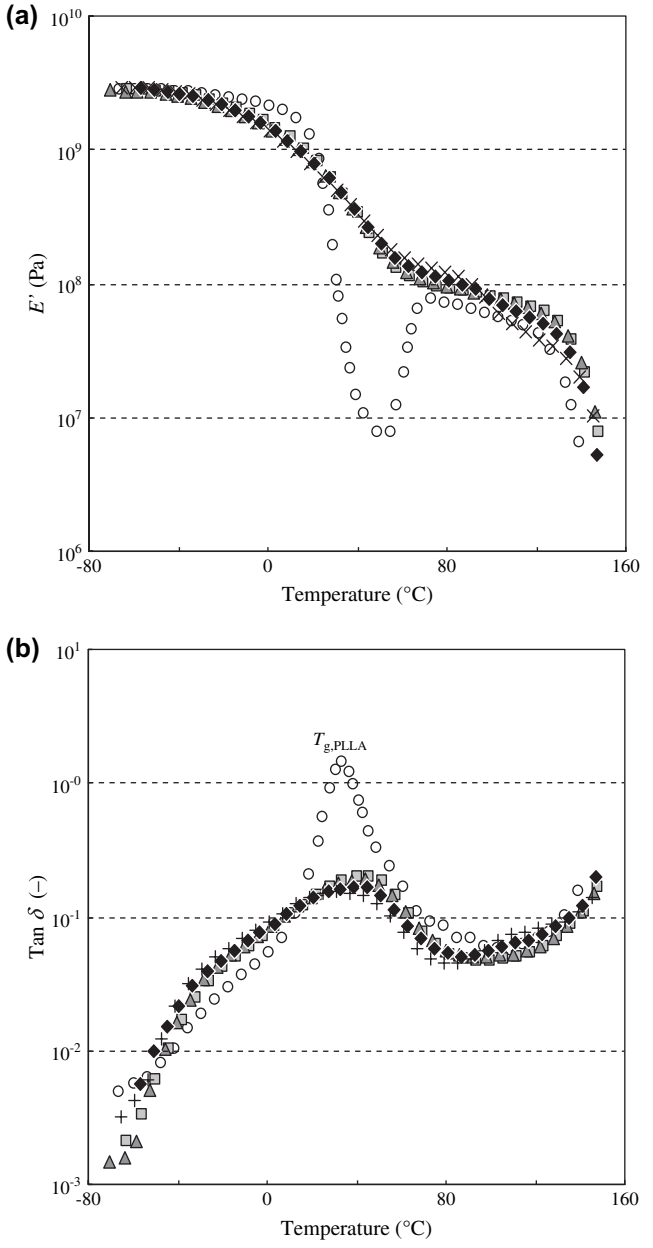

Fig. 4. Dynamic viscoelastic curves of PLLA/RKM20 and PLLA/PBSL/RKM20: (a) E' and (b) tan δ. The PLLA/PBSL weight ratio: ○ − 100/0, ■ − 99/1, ▲ − 95/1, ◆ − 90/10, × − 80/20.

100/0 to 80/20. This result suggests that the compatibility of PLLA and PBSL may be improved by the addition of 10 wt% RKM, or the concentration of RKM in the PLLA-rich phase may be higher than that in the PBSL-rich phase. Judging from the following FE-SEM result, it is thought that the latter factor contributes. The temperature where E' starts to rise due to crystallization of PLLA component shifted to a lower temperature region by the addition of PBSL to PLLA/PBSL/RKM10 blends, indicating that the addition of PBSL enhances the cold crystallization of PLLA. In the case of PLLA/PBSL/RKM20, a rise of E' due to the crystallization of PLLA component was not observed, suggesting that the injection molded sample before the dynamic viscoelastic measurement has already attained almost the ultimate crystallinity. The crystallization enhancement effect due to the addition of RKM and PBSL is discussed in the following section. The tan δ peak of PLLA/PBSL/RKM20 is much weaker and broader than that of PLLA/RKM20, indicating that the former blend has a higher crystallinity than the latter blend and that the amorphous PLLA-rich phase of the former blend composed of some components with different mobilities. The $T_{g,PLLA}$ calculated from the temperature at the maximum of tan δ peak for PLLA/PBSL5/RKM20 is higher than that for PLLA/RKM20 (Table 1). It is thought that the mobility of amorphous PLLA-rich phase is disturbed by the presence of highly crystallized PLLA lamella. The broadening of the tan δ peak may be due to a heterogeneous distribution of RKM induced by the crystallization of PLLA component or some compatibilization of PLLA-rich phase and PBSL-rich phase.

3.2. Morphologies by FE-SEM

Fig. 5 shows the FE-SEM micrographs of PLLA/PBSL, PLLA/PBSL/RKM10 and PLLA/PBSL/RKM20 blends. The PLLA/PBSL and PLLA/PBSL/RKM10 blends appeared as phase-separated system where PBSL-rich phase dispersed as fine particles, in agreement with the result of dynamic viscoelastic measurement. Because the interface of PLLA-rich phase and PBSL-rich phase is not so clear for PLLA/PBSL/RKM20, it is thought that the compatibility between the two phases is somewhat improved for PLLA/PBSL/RKM20 blend compared with PLLA/PBSL/RKM10 and PLLA/PBSL. This result is related to the broad tan δ peak observed in Fig. 4.

3.3. Tensile properties

Fig. 6 shows the tensile properties of PLLA/PBSL and PLLA/PBSL/RKM blends. Regarding the blends without PBSL, the addition of 10 wt% RKM to PLLA resulted in little increase of elongation at break and slight decrease of modulus. When 20 wt% RKM is added, a considerable increase of the elongation and decrease of modulus occurred. This result indicates that the addition of 20 wt% RKM is necessary to get a

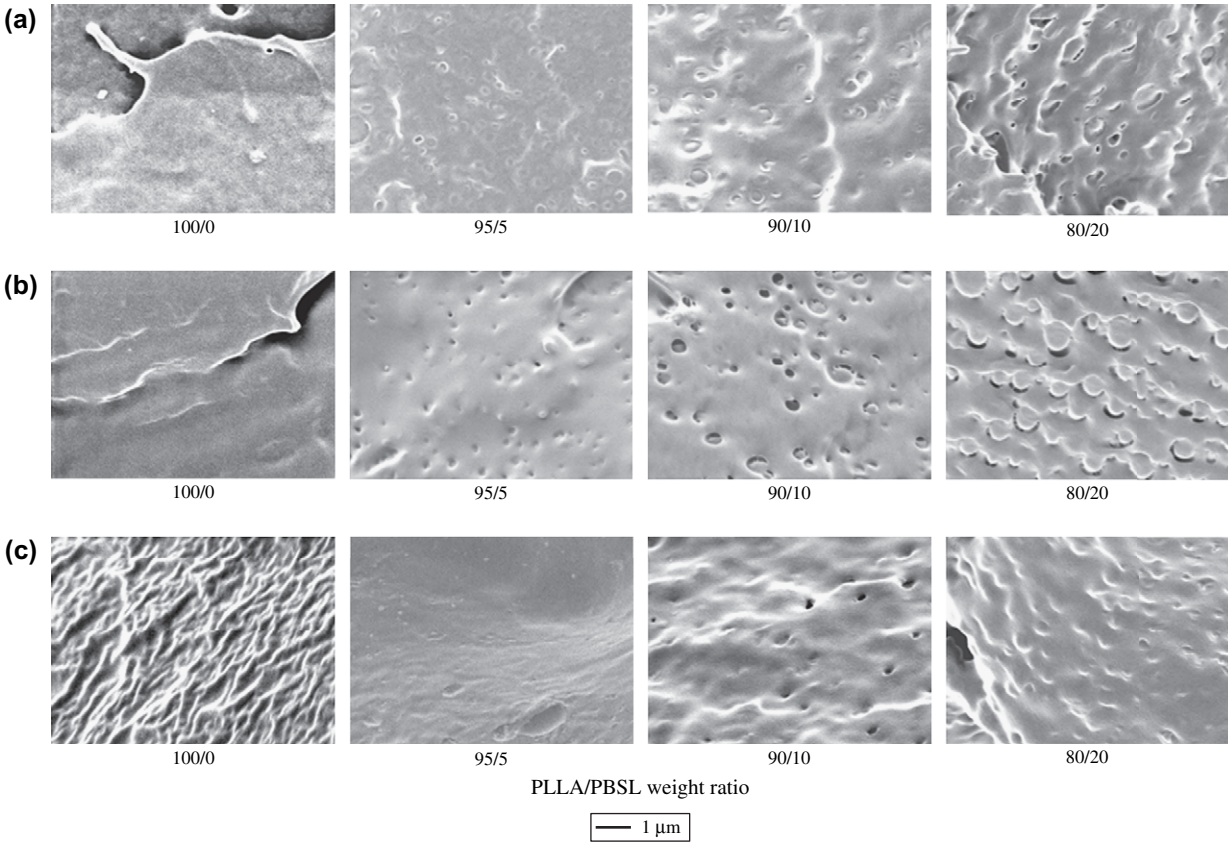

Fig. 5. FE-SEM images of: (a) PLLA/PBSL, (b) PLLA/PBSL/RKM10, and (c) PLLA/PBSL/RKM20.

good plasticizing effect. When PBSL is added to the PLLA/RKM20, the elongation slightly decreased, and modulus slightly increased, due to the increase of the degree of crystallization mentioned above. It is noteworthy that addition of slight amount of PBSL to PLLA/RKM10 can assist the plasticizing effect to give the materials having a good flexibility as is obvious from the typical stress–strain curves shown in Fig. 7.

3.4. Non-isothermal crystallization behavior by DSC

First, non-isothermal crystallization behavior of the PLLA component at a cooling stage from the melted state of PLLA/PBSL/RKM at 190 °C for 3 min was monitored by DSC. Fig. 8 shows typical cooling DSC thermograms at cooling rates of 1, 5, and 20 °C/min for PLLA/RKM20 and PLLA/PBSL5/RKM20. The DSC parameters of all the samples

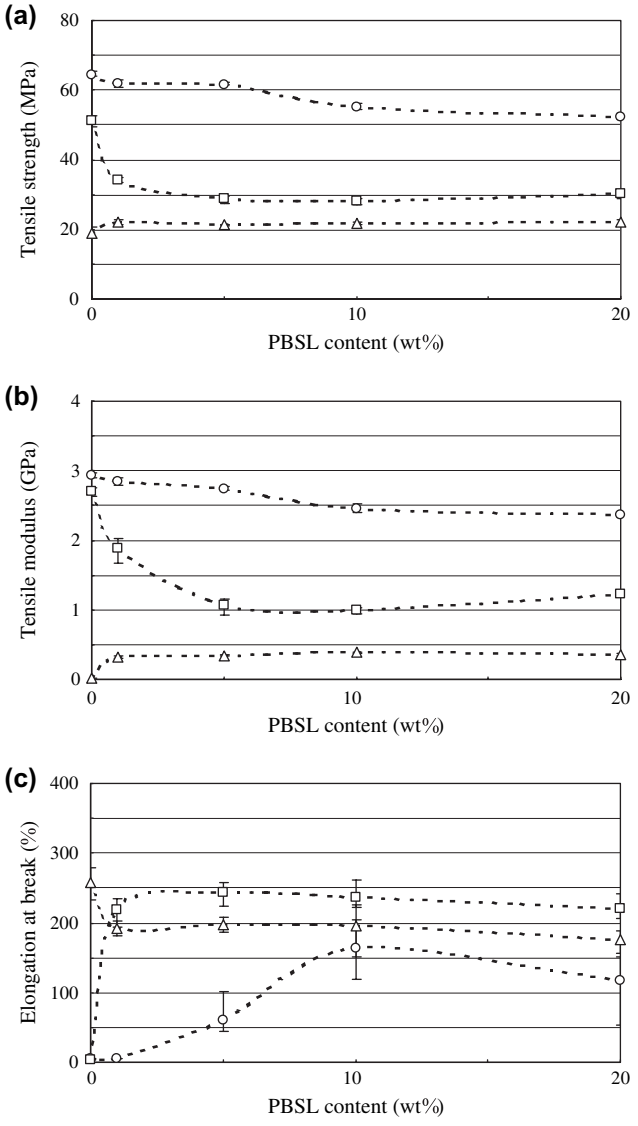

Fig. 6. Tensile properties of PLLA/PBSL and PLLA/PBSL/RKM: (a) tensile strength, (b) tensile modulus, and (c) elongation at break. RKM content: ○ – 0 wt%, □ – 10 wt%, △ – 20 wt%.

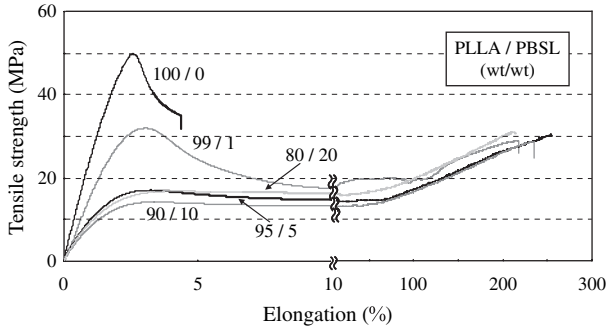

Fig. 7. Typical stress–strain curves for PLLA/RKM10 and PLLA/PBSL/RKM10.

obtained from the cooling thermograms are summarized in Table 2. All the samples showed no exothermic peak due to the crystallization of the PLLA component at a cooling rate of 20 °C/min. When the cooling rate is 5 °C/min, the PLLA crystallization similarly did not occur for PLLA. However, an exothermic peak due to the crystallization of PLLA ($T_{c,PLLA}$) was observed for PLLA/RKM and PLLA/PBSL/RKM. The $T_{c,PLLA}$ decreased with increasing amount of RKM, while rose by the addition of PBSL. The heat of crystallization per *g*-PLLA ($\Delta H_{c,PLLA}$) increased with increasing amount of RKM and by the addition of PBSL. This result suggests that both RKM and PBSL enhance the crystallization of PLLA, and that their mechanism of crystallization enhancement is different.

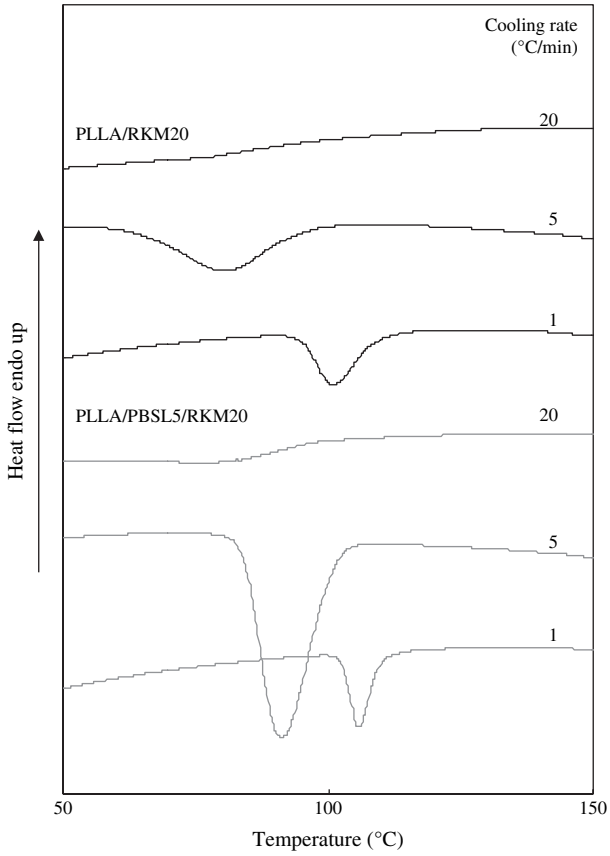

Fig. 8. The cooling DSC thermograms for the PLLA/RKM20 and PLLA/PBSL5/RKM20 blends after melted at 190 °C for 3 min.

Table 2
DSC parameters obtained from the first cooling scan for the PLLA/PBSL/RKM blends after melted at 190 °C for 3 min

Blend	Cooling rate (°C/min)	$T_{c,PLLA}$ (°C)	$\Delta H_{c,PLLA}$ (J/g)	$\chi_{c,PLLA}$ (%)
PLLA	20	–	–	–
	5	–	–	–
	1	107.5	25.1	27.0
PLLA/PBSL5	20	–	–	–
	5	100.2	13.8	14.8
	1	115.0	38.9	41.8
PLLA/RKM10	20	–	–	–
	5	88.5	2.56	2.75
	1	104.6	35.0	37.6
PLLA/PBSL5/RKM10	20	–	–	–
	5	93.2	26.8	28.8
	1	110.1	35.6	38.2
PLLA/RKM20	20	–	–	–
	5	80.3	14.3	15.3
	1	100.9	31.9	34.3
PLLA/PBSL5/RKM20	20	–	–	–
	5	91.3	33.6	36.1
	1	105.8	34.9	37.5

Next, the cold-crystallization behavior of all the blends at the second heating stage was investigated using the samples quenched at a cooling rate of 100 °C/min after melted at 190 °C for 3 min. In the cooling stage of quenching, no exothermic peak due to crystallization of the PLLA component was observed, while the crystallization of the PBSL component occurred. Fig. 9 shows the second heating scan for PLLA/PBSL/RKM20 blends at a rate of 20 °C/min. Table 3 summarizes the DSC parameters obtained from this heating run for all the samples. As a general trend, the cold-crystallization temperature for PLLA component ($T'_{c,PLLA}$) shifted to a lower temperature region, and its enthalpy $\Delta H'_{c,PLLA}$ increased by the addition of small amount of PBSL (1 and 5 wt%). Also, the similar shift of $T'_{c,PLLA}$ and $\Delta H'_{c,PLLA}$ was observed in the case of the addition of RKM. These results suggest that the addition of PBSL and RKM enhances the cold crystallization of PLLA component. The addition of PBSL more than 5 wt% did not cause a further crystallization enhancement, because the increase of $T'_{c,PLLA}$ and the decrease of $\Delta H'_{c,PLLA}$ are observed for some samples with the PLLA/PBSL weight ratio 90/10 and 80/20. However, because the exothermic peaks due to crystallization of PLLA should overlap with the endothermic peak due to melting of PBSL, the values of $T'_{c,PLLA}$ and $\Delta H'_{c,PLLA}$ at a high PBSL content may be inaccurate. Regarding the melting temperature (T_m) of PLLA component, although the addition of PBSL had little influence on the T_m, the addition of RKM caused a considerable decrease of the T_m, which became a double melting peak. The PLLA crystals rapidly formed under the heterogeneous nucleation at a heating process may become more imperfect in the presence of RKM. Regarding T_g of the PLLA-rich phase of the quenched PLLA/PBSL/RKM blends, although the T_g slightly decreased with increasing amount of PBSL for the blends with RKM content 0 and 10 wt%, a significant decrease of T_g was observed for the blends with RKM content 20 wt%. This result is in agreement with the observation of some

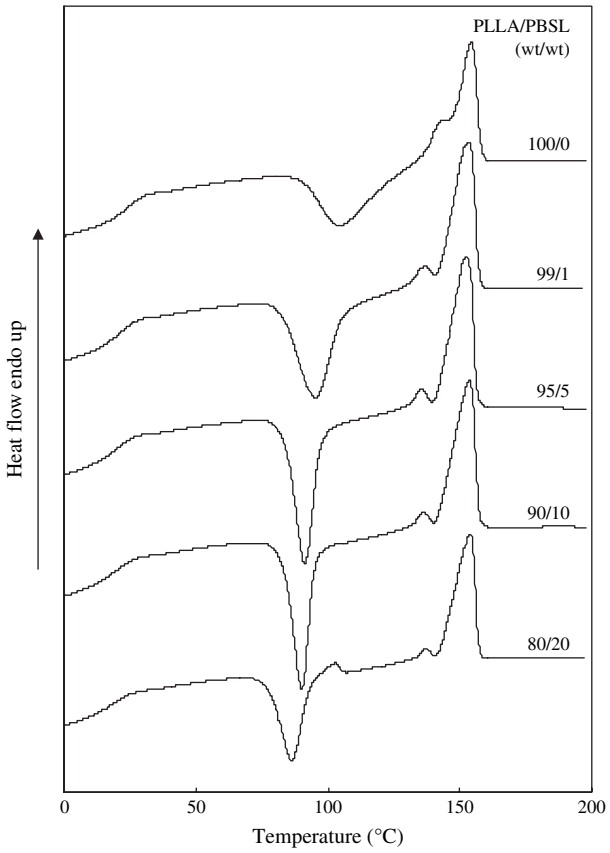

Fig. 9. The second heating DSC thermograms at a heating rate of 20 °C/min for the PLLA/PBSL/RKM20 blends quenched at a cooling rate of 100 °C/min after melted at 190 °C for 3 min.

Table 3
DSC parameters obtained from the second heating scan for the PLLA/PBSL/RKM blends after quenched at a cooling rate of 100 °C/min from the melt

RKM content (wt%)	PLLA/PBSL weight ratio	PLLA component				
		T_g (°C)	T'_c (°C)	$\Delta H'_c$ (J/g)	T_m (°C)	ΔH_m (J/g)
0	100/0	60.5	136.3	6.38	164.5	7.02
	99/1	59.4	132.0	23.1	162.8	25.3
	95/5	58.2	124.2	33.2	162.4	38.1
	90/10	58.1	127.3	28.4	163.8	31.6
	80/20	59.0	128.3	29.6	164.1	30.9
10	100/0	40.0	120.5	22.3	154.7/160.4	28.9
	99/1	39.5	121.5	23.0	155.3/160.7	28.0
	95/5	37.4	107.1	34.7	148.6/159.3	40.2
	90/10	37.0	99.7	30.5	146.3/158.7	34.7
	80/20	38.5	105.4[a]	32.6[a]	149.3/159.7	38.8
20	100/0	25.0	104.8	31.1	142.3/154.4	34.3
	99/1	22.6	95.4	35.1	136.3/153.4	41.5
	95/5	20.6	91.4	33.7	135.6/152.4	40.9
	90/10	21.2	90.0	31.1	136.3/153.7	40.0
	80/20	18.6	86.3[a]	26.3[a]	137.3/154.4	36.1

[a] The separation of the exothermic peaks due to cold crystallization of PLLA and PBSL components and the endothermic peak due to melting of PBSL is not sufficient.

compatibilization of PLLA-rich phase and PBSL-rich phase by the FE-SEM.

3.5. Isothermal crystallization behavior by DSC

The isothermal crystallization behavior of the PLLA component was monitored at 90–120 °C by DSC after the PLLA/PBSL/RKM blends were melted at 190 °C for 3 min. The isothermal crystallization kinetics of the blend was analyzed by means of Avrami equation:

$$\chi_c(t)/\chi_c(\infty) = 1 - \exp(-kt^n) \quad (2)$$

where k is the rate constant of crystallization and n is the Avrami exponent, which can be related to the type of nucleation and to the geometry of crystal growth. From the intercepts and the slopes of the plots of $\log[-\ln(1-\chi_c(t)/\chi_c(\infty))]$ *versus* $\log t$, the values of k and n were calculated, respectively; all these values are summarized in Table 4. As each curve has a linear portion followed by a gentle roll-off at longer times, the slope at the shorter crystallization time corresponding to primary crystallization was adopted. The obtained n for pure PLLA was 2.4–2.7, which should be three-dimensional crystal growth assuming heterogeneous nucleation. Some crystalline nuclei are thought to remain at the melting at 190 °C for 3 min. Relation between crystallization temperature (T_c) and crystallization half-time ($t_{1/2}$), the time at which the relative degree of crystallization is 0.5, is shown in Fig. 10. The addition of PBSL to PLLA or PLLA/RKM caused the shortening of $t_{1/2}$ and the increase of k and n over the whole crystallization temperatures, although there is some exception. As was already reported, it is interesting that the addition of PBS whose structure is analogous to PBSL is ineffective on the shortening of $t_{1/2}$ [22]. On the other hand, the addition of RKM to PLLA or PLLA/PBSL5 was more effective on the shortening of $t_{1/2}$ and increase of k at a lower crystallization temperature. The $t_{1/2}$s of PLLA/PBSL5/RKM10 and PLLA/PBSL5/RKM20 were rather longer than that of PLLA/PBSL5 at T_c 110–120 °C. The value of n became a little smaller by the addition of 10 wt% RKM to PLLA or PLLA/PBSL5, although there is some exception.

Fig. 11 shows polarizing optical micrographs of the PLLA/PBSL/RKM films annealed at 110 °C as a function of time. Obviously, the addition of RKM caused a decrease of the number of PLLA spherulites, suggesting that the increase of PLLA chain mobility due to a plasticizing effect of RKM disturbs the formation of crystalline nucleus. On the other hand, the addition of PBSL caused an increase of the number of spherulites, suggesting that PBSL becomes

Table 4
Isothermal crystallization parameters for PLLA/PBSL/RKM blends

Blend	Crystallization temperature (°C)	$t_{1/2}$ (min)	k (s^{-n})	n	$\chi_{c,PLLA}$ (%)
PLLA	90	20.10	2.42×10^{-8}	2.42	13.3
	95	10.15	3.99×10^{-8}	2.60	30.4
	100	11.10	5.32×10^{-8}	2.52	29.8
	105	8.76	3.33×10^{-8}	2.69	42.6
	110	12.50	2.47×10^{-8}	2.59	38.6
	115	13.30	2.95×10^{-8}	2.54	38.9
	120	19.30	4.91×10^{-9}	2.66	39.1
PLLA/PBSL5	90	8.17	1.24×10^{-8}	2.88	28.8
	95	5.50	7.76×10^{-8}	2.76	34.0
	100	4.75	1.73×10^{-7}	2.69	33.2
	105	3.99	2.92×10^{-7}	2.68	41.5
	110	4.15	2.48×10^{-7}	2.69	41.4
	115	3.97	1.37×10^{-7}	2.82	41.2
	120	5.70	1.37×10^{-8}	3.04	43.0
PLLA/RKM10	90	7.00	4.47×10^{-7}	2.36	32.5
	95	4.80	4.15×10^{-7}	2.53	36.4
	100	4.90	6.21×10^{-7}	2.45	38.5
	105	7.05	2.40×10^{-7}	2.46	41.2
	110	9.05	1.01×10^{-7}	2.50	41.5
	115	12.46	8.12×10^{-8}	2.76	43.6
	120	21.12	5.53×10^{-9}	2.61	48.2
PLLA/PBSL5/RKM10	90	3.37	7.01×10^{-7}	2.60	33.9
	95	2.84	7.63×10^{-7}	2.67	35.6
	100	2.73	6.57×10^{-7}	2.73	36.5
	105	3.29	5.94×10^{-7}	2.74	37.3
	110	5.92	1.70×10^{-7}	2.88	41.3
	115	9.59	1.09×10^{-8}	3.06	48.7
	120	20.30	2.33×10^{-10}	3.07	44.7
PLLA/RKM20	90	3.11	1.46×10^{-6}	2.50	32.5
	95	3.36	7.07×10^{-7}	2.60	36.4
	100	5.53	2.90×10^{-7}	2.53	38.5
	105	6.75	9.62×10^{-8}	2.63	41.2
	110	12.98	3.35×10^{-8}	2.53	41.5
	115	22.03	1.56×10^{-8}	2.45	43.6
PLLA/PBSL5/RKM20	90	1.73	1.36×10^{-6}	2.83	33.9
	95	1.63	1.69×10^{-6}	2.82	35.6
	100	1.94	1.03×10^{-6}	2.82	36.5
	105	2.79	2.01×10^{-7}	2.94	37.3
	110	6.55	2.80×10^{-8}	2.85	41.3
	115	22.25	1.60×10^{-8}	2.44	48.7

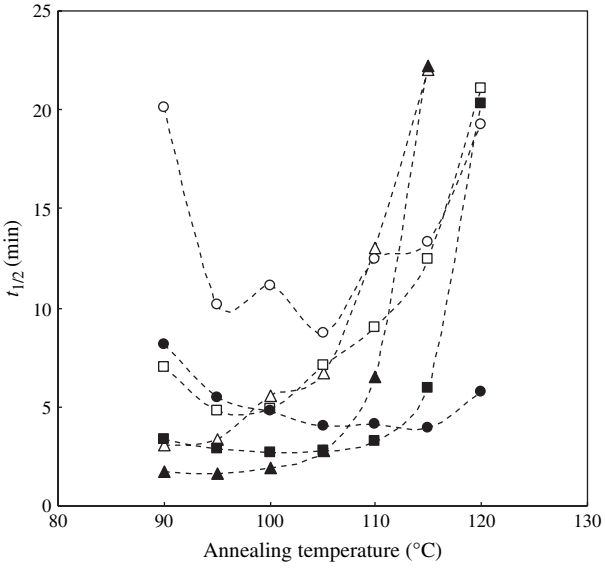

Fig. 10. Half crystallization time ($t_{1/2}$) as a function of crystallization temperature for PLLA/PBSL/RKM: ○ – PLLA, □ – PLLA/RKM10, △ – PLLA/RKM20, ● – PLLA/PBSL5, ■ – PLLA/PBSL5/RKM10, ▲ – PLLA/PBSL5/RKM20.

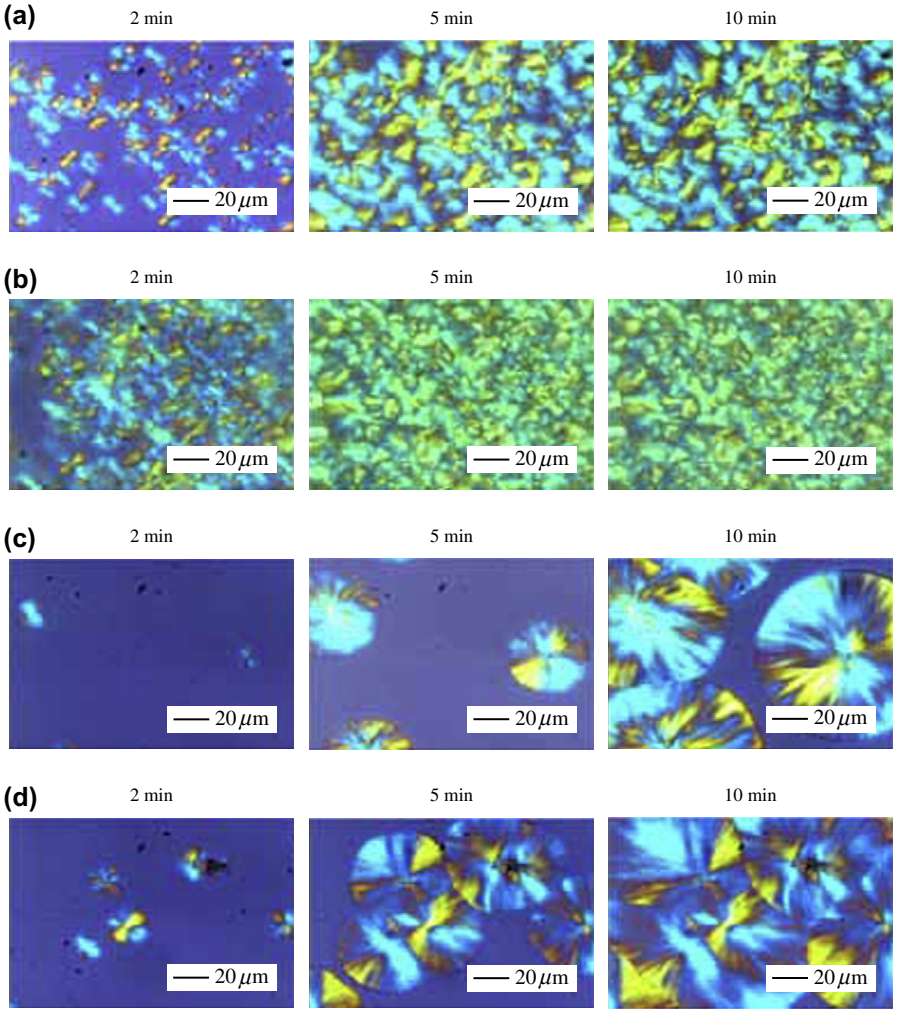

Fig. 11. Photomicrographs of the films annealed at 110 °C from the melt: (a) PLLA/RKM10, (b) PLLA/PBSL5/RKM10, (c) PLLA/RKM20, and (d) PLLA/PBSL5/RKM20.

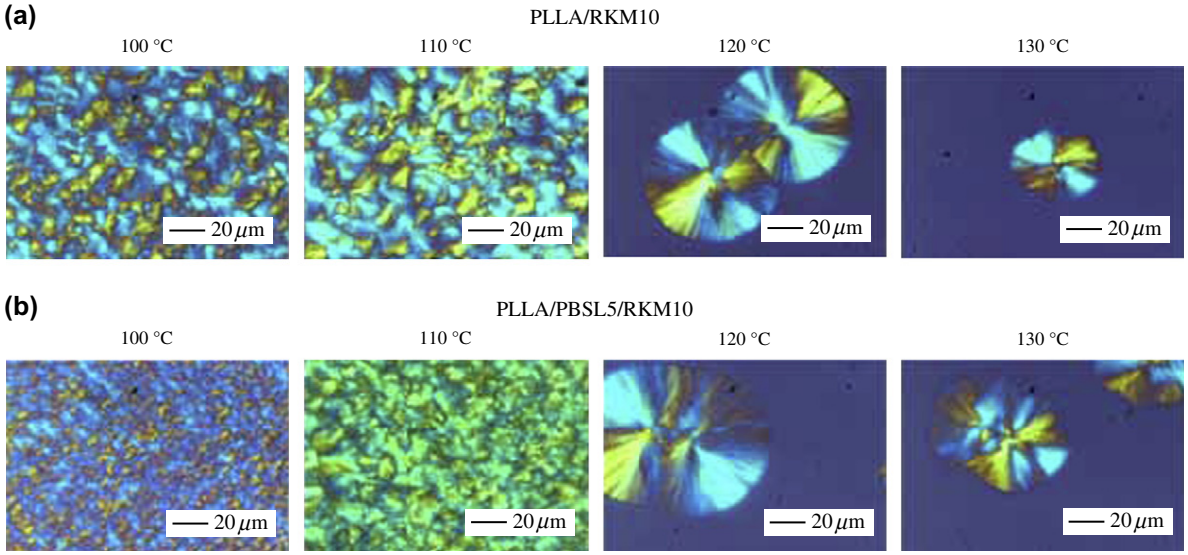

Fig. 12. Photomicrographs of the films annealed at various temperatures for 10 min from the melt: (a) PLLA/RKM10 and (b) PLLA/PBSL5/RKM10.

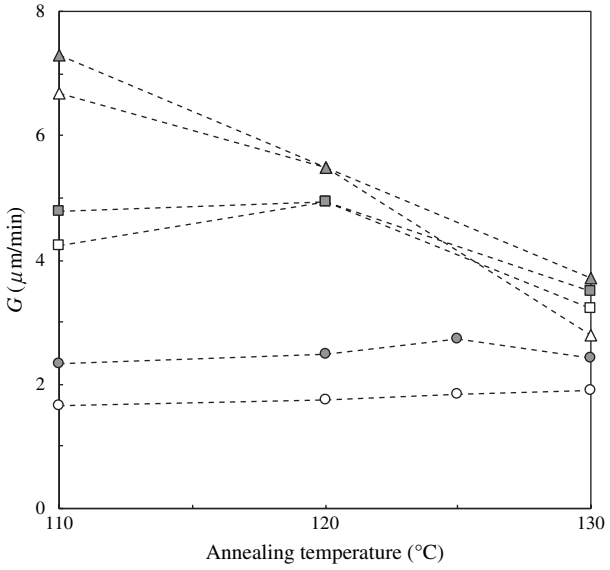

Fig. 13. Growth rate of spherulite radius as a function of annealing temperature for PLLA/PBSL/RKM blends: ○ – PLLA, □ – PLLA/RKM10, △ – PLLA/RKM20, ● – PLLA/PBSL5, ■ – PLLA/PBSL5/RKM10, ▲ – PLLA/PBSL5/RKM20.

a crystal nucleator at 110 °C, which is very close to T_m of PBSL (109.8 °C). Fig. 12 shows polarizing optical micrographs of PLLA/RKM10 and PLLA/PBSL5/RKM10 films annealed at various temperatures for 10 min. The number of spherulites decreased with increasing annealing temperature. Although the number of spherulites of PLLA/PBSL5/RKM10 is larger than that of PLLA/RKM10 at 100 and 110 °C, there is little difference in the number at 120 and 130 °C. This result indicates that PBSL is not an effective nucleator at a higher temperature region around 120–130 °C, as is easily supposed from the fact that PBSL is in a liquid phase at the temperature range. Therefore, it is supposed that the addition of biodegradable polymers (for example, poly(ε-caprolactone): $T_m = 52.5$ °C) with the T_m much lower than PBSL is ineffective on the PLLA nucleation. Fig. 13 shows the growth rate (G) of spherulite radius as a function of annealing temperature. The G increases with increasing RKM content. This effect is more prominent at a lower annealing temperature, suggesting that the PLLA chain mobility is an important factor for the crystal growth. From this viewpoint, the plasticizer with a low molecular weight such as RKM should be a good accelerator of PLLA crystal growth. The addition of PBSL to PLLA or PLLA/RKM caused a little increase of G, suggesting that the PBSL slightly dissolved in PLLA causes a little increase of the PLLA chain mobility.

4. Conclusions

The PLLA blends with various compositions of PBSL and RKM were prepared by melt-mixing and subsequent injection molding, and their mechanical properties, morphology, and crystallization behavior were compared. FE-SEM measurement revealed that the PLLA/PBSL and PLLA/PBSL/RKM blends are finely dispersed immiscible blends. In the case of PLLA/PBSL5/RKM20, some compatibilization of PLLA-rich and PBSL-rich phases was observed. The addition of a slight amount of PBSL to PLLA/RKM10 can assist the plasticizing effect to give the materials having a good flexibility. As a result of investigation of the crystallization behavior, it was revealed that the addition of RKM to PLLA causes the enhancement of crystalline growth rate at a lower T_c, and the addition of PBSL mainly enhances the formation of crystal nucleus. As a whole, the PLLA/PBSL5/RKM10 blend is thought to be a promising material for a packaging application having a good flexibility and a relatively rapid crystallization rate at the crystallization temperature 90–110 °C.

References

[1] Vink ETH, Rabago KR, Glassner DA, Gruber PR. Polym Degrad Stab 2003;80(3):403–19.
[2] Sawyer DJ. Macromol Symp 2003;201:271–81.
[3] Scott A, Sissell K. Chem Week 2003;165(3):18.
[4] Inoue Y. Foods Food Ingred J Jpn 2003;208(8):648–54.
[5] Ohara H. J Appl Glycosci 2003;50(3):405–10.
[6] Warmington A. Eur Plast News 2001;28(5):49–50.
[7] Garlotta D. J Polym Environ 2001;9(2):63–84.
[8] Ohara H. Health Digest 1999;14(1):1.
[9] Hu Y, Hu YS, Topolkaraev V, Hiltner A, Baer E. Polymer 2003;44(19):5681–9.
[10] Kulinski Z, Piorkowska E. Polymer 2005;46(23):10290–300.
[11] Ljungberg N, Wesslen B, Andersson T. J Appl Polym Sci 2003;88(14):3239–47.
[12] Martin O, Averous L. Polymer 2001;42(14):6209–19.
[13] Jacobsen S, Fritz HG. Polym Eng Sci 1999;39(7):1303–10.
[14] Shibata M, Someya Y, Orihara M, Miyoshi M. J Appl Polym Sci 2006;99(5):2594–602.
[15] Takagi J, Nemoto T, Takahashi T, Taniguchi T, Koyama K. Seikei-Kakou 2003;15(8):581–7.
[16] Park JW, Im SS. J Appl Polym Sci 2002;86:647–55.
[17] Yang JM, Chen HL, You JW, Hwang JC. Polym J 1997;29(8):657–62.
[18] Tsuji H, Ikada Y. J Appl Polym Sci 1998;67(3):405–15.
[19] Tamura N, Chitose T, Komai K, Takahasi S, Kssemura T, Obuchi S. Trans Mater Res Soc Jpn 2004;29(5):2017–20.
[20] Ohkoshi I, Abe H, Doi Y. Polymer 2000;41(15):5985–92.
[21] Koyama Y, Doi Y. Polymer 1997;38(7):1589–93.
[22] Shibata M, Inoue Y, Miyoshi M. Polymer 2006;47(10):3557–64.